This document was prepared in conjunction with work accomplished under Contract No. DE-AC09-96SR18500 with the U.S. Department of Energy.

Proceedings of PVP2008
2008 ASME Pressure Vessels and Piping Division Conference
July 27-31, 2008, Chicago, Illinois

PVP2008-61608

PREDICTION OF CHARACTERISTIC LENGTH AND FRACTURE TOUGHNESS IN DUCTILE-BRITTLE TRANSITION

Z. X. Wang
Engineering Mechanics
Jiangsu University
Zhenjiang, Jiangsu, China
wzx-5566 @163.com

H. M. Li
Engineering Mechanics
Jiangsu University
Zhenjiang, Jiangsu, China
lihuimei23@163.com

Y. J. Chao
Department of Mechanical Engineering
University of South Carolina
Columbia, SC 29208, USA
chao@engr.sc.edu

P. S. Lam
Materials Science and Technology
Savannah River National Laboratory
Aiken, SC 29808, USA
ps.lam@srnl.doe.gov

ABSTRACT

Finite element method was used to analyze the three-point bend experimental data of A533B-1 pressure vessel steel obtained by Sherry, Lidbury, and Beardsmore [1] from -160 to -45 °C within the ductile-brittle transition regime. As many researchers have shown, the failure stress (σ_f) of the material could be approximated as a constant. The characteristic length, or the critical distance (r_c) from the crack tip, at which σ_f is reached, is shown to be temperature dependent based on the crack tip stress field calculated by the finite element method. With the J-A_2 two-parameter constraint theory in fracture mechanics, the fracture toughness (J_C or K_{JC}) can be expressed as a function of the constraint level (A_2) and the critical distance r_c. This relationship is used to predict the fracture toughness of A533B-1 in the ductile-brittle transition regime with a constant σ_f and a set of temperature-dependent r_c. It can be shown that the prediction agrees well with the test data for wide range of constraint levels from shallow cracks (a/W= 0.075) to deep cracks (a/W= 0.5), where a is the crack length and W is the specimen width.

INTRODUCTION

Many pressure vessel and piping components are typically designed so the materials of construction exhibit ductile behavior during the normal operating temperatures. As the temperature decreases under abnormal condition, these materials may experience ductile-brittle transition resulting in a change of fracture mode and a reduction of fracture toughness. Therefore, for material selection criteria and structural integrity assessment under various operating conditions, it is desirable to understand the fracture mechanism during the ductile-brittle transition and to be able to predict the temperature-dependent fracture toughness.

During the ductile-brittle transition in low alloy steels, the fractography changes from a fracture strain (ε_f)-controlled plastic dimple fracture to a critical stress (σ_f)-controlled cleavage mode. Based on the model proposed by Richie, Knott, and Rice (RKR) [2,3], brittle fracture occurs when the stress state exceeds σ_f at a characteristic distance (r_c) about twice the grain size away from the crack tip. Further investigation showed that, even the cleavage fracture mechanism during ductile-brittle transition may change with the specimen geometry, temperature, loading rate, prestrain, and material composition, it appears that σ_f is a stable quantity and may be used as a material toughness parameter [4-8].

The fracture behavior of A533B-1 pressure vessel steel was investigated by Sherry, Lidbury, and Beardsmore [1] using three-point bend specimens with various crack length (a) to width (W) ratios (a/W= 0.075, 0.1, 0.2, and 0.5) within the temperature range between -160 and -45 °C. Using the fracture toughness data of a/W= 0.5, a master curve (K_{JC}) can be constructed as a function of temperature. With ±5% range of a constant σ_f suggested by Chen, Zhen, and Chao [9], r_c as a function of temperature can be determined by the finite element method. By applying the temperature-dependent r_c with the J-A_2 constraint theory in fracture mechanics, the fracture toughness for specimens with any a/W ratios can be calculated at each temperature. It is found that the predicted K_{JC} values agree well with those obtained by Sherry et al. [1] for a/W= 0.075, 0.1, 0.2, and 0.5 within the temperature range from -160 to -45 °C.

MATERIAL PROPERTIES AND FINITE ELEMENT MODEL

The elastic-plastic material response is assumed to follow the Ramberg-Osgood power law strain hardening function

$$\frac{\varepsilon}{\varepsilon_0} = \frac{\sigma}{\sigma_0} + \alpha\left(\frac{\sigma}{\sigma_0}\right)^n \tag{1}$$

in which σ is the stress, ε is the strain, σ_o is the yield stress, E is the Young's modulus, n is the strain hardening exponent, α is a material constant, and the corresponding yield strain ε_o is defined as σ_o/E.

It is well known that A533B-1 is a very ductile material. However, as the temperature decreases, the material exhibits ductile to brittle transition, that is, the fracture surface on the upper shelf shows ductile tearing and dimple fracture, while on the lower shelf the cleavage fracture dominates. In the transition regime, the microstructures appear to be cleavage with indication of microvoids. For the current study, the material properties and fracture test data for A533B-1 are based on the work by Sherry et al. [1]. By regression analyses, the test data in term of temperature (T, in Celsius) can be expressed as (see Figs. 1(a) to 1(c) and also in Reference [1]):

$$\sigma_0 = 0.0074T^2 - 0.2386T + 493.1278 \quad \text{(MPa)} \tag{2}$$

$$E = -0.0511T + 209.9588 \quad \text{(GPa)} \tag{3}$$

$$n = 0.0005T^2 + 0.0359T + 10.9330 \tag{4}$$

Note that in the original report by Sherry et al. [1], a constant n= 12 was used instead of Eq. (4). The coefficient α in Eq. (1) is unity (1.0) in the present work.

The width (W) and the thickness (B) for test specimens with a/W= 0.1, 0.2 and 0.5 are, respectively, 134 mm and 67 mm. In the case of the shallow crack specimens (a/W= 0.075), the width and the thickness are both 50 mm. Therefore, using the weakest link statistical theories and following the American Society for Testing and Materials (ASTM) E 1921, "Standard Test Method for Determination of Reference Temperature, T_o, for Ferritic Steels in the Transition Range [12]," the fracture toughness (J_C or K_{JC}) from Reference [1] can be converted to that for the standard 1T specimen, for which the thickness B_{1T}= 25.4 mm or 1 inch:

$$K_{JC(1T)} = K_{min} + [K_{JC} - K_{min}]\left(\frac{B}{B_{1T}}\right)^{1/4} \tag{5}$$

$$K_{JC} = \sqrt{J_C E / (1-\nu^2)} \tag{6}$$

where $K_{JC(1T)}$ is the fracture toughness for the 1T specimen and K_{min}= 20 MPa $m^{1/2}$. Figure 1(d) shows the dependencies of 1T fracture toughness on specimen geometry (a/W) and temperature (T).

The ABAQUS finite element program [10] was used to analyze various specimens tested by Sherry et al. [1]. Due to geometric and loading symmetries, only one-half of the specimen is modeled. The eight-noded reduced integration elements were used in the calculation. Figures 2a and 2b show the typical finite element meshes for a/W= 0.1 and 0.5, respectively. The smallest element size near the crack tip is 0.002 mm. The concentrated load acting on the simply-supported three-point bend specimen is applied to the end of the uncracked ligament.

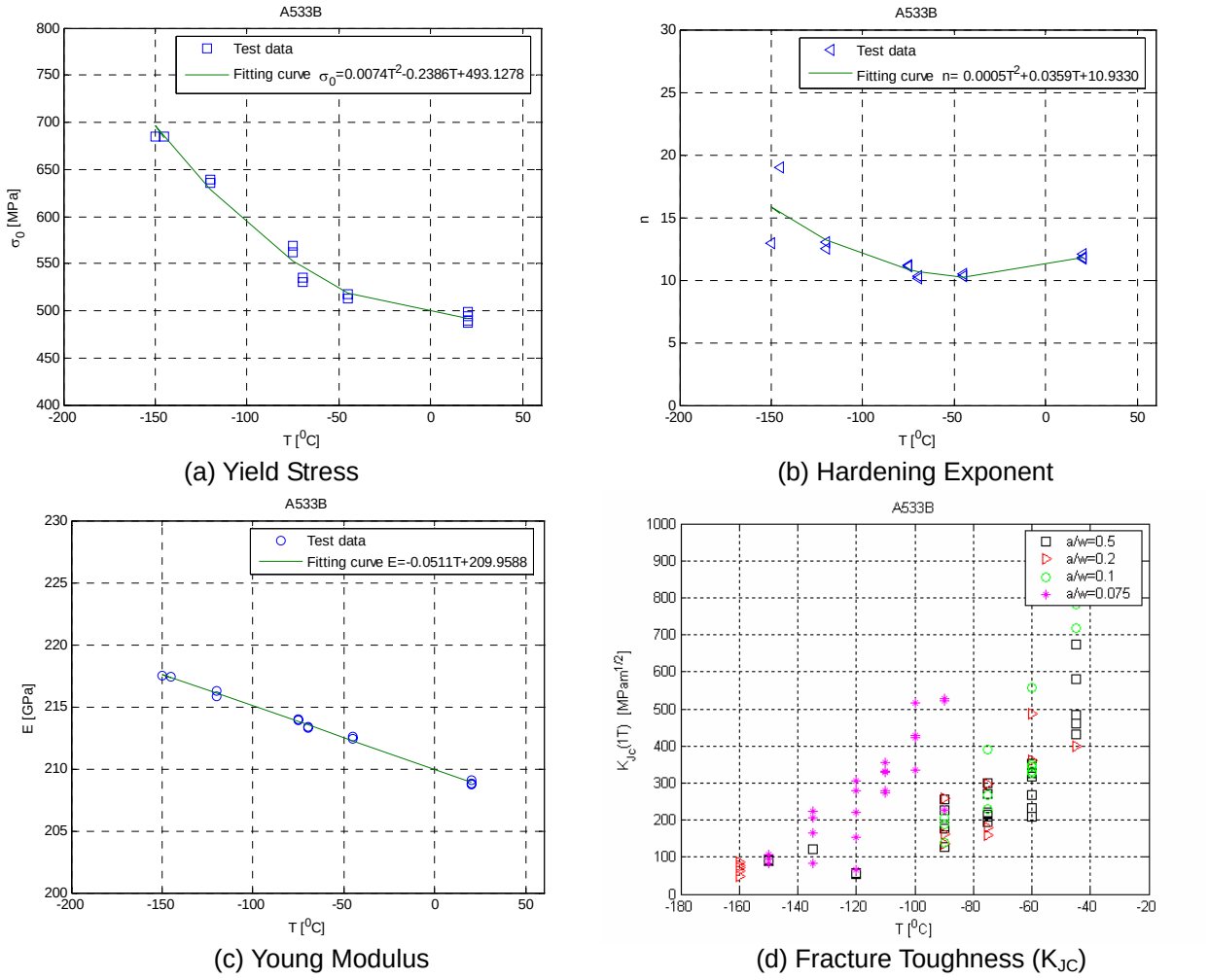

(a) Yield Stress

(b) Hardening Exponent

(c) Young Modulus

(d) Fracture Toughness (K_{JC})

Figure 1 Temperature dependent material properties (a) yield stress, (b) hardening exponent, (c) Young's modulus, and (d) fracture toughness (K_{JC}). Test data were reported by Sherry, et al. [1].

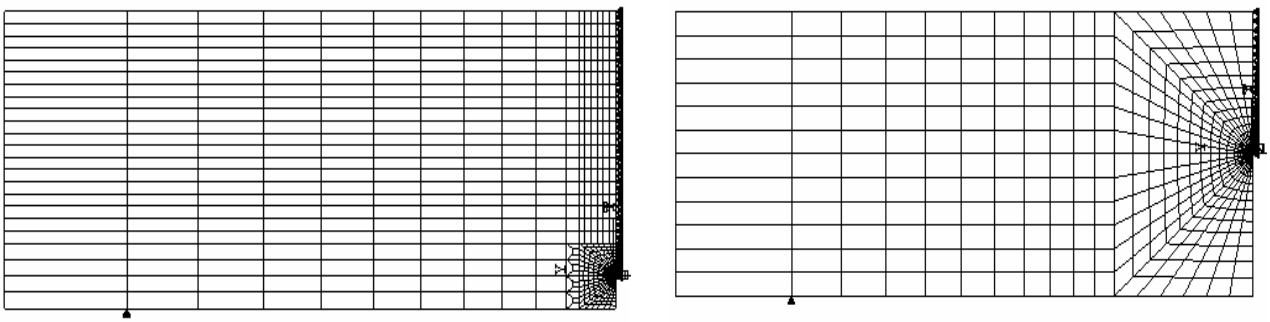

(a) a/W= 0.1

(b) a/W= 0.5

Figure 2 Finite element models for (a) shallow crack (a/W= 0.1) and (b) deep crack (a/W= 0.5)

DETERMINATION OF CHARACTERISTIC DISTANCE (r_c)

The fracture toughness obtained from material testing typically exhibits large data scattering in the ductile-brittle transition regime. The statistically-formulated master curve method has been adopted as a major approach to describe the fracture toughness for ferritic materials [11]. Based on ASTM E 1921 [12], the master curve for the 1T specimen is given as

$$K_{JC(1T)} = 30 + 70e^{0.019(T-T_o)} \quad (7)$$

where $K_{JC(1T)}$ is in MPa $m^{1/2}$, T is the temperature in °C, and T_o is a reference temperature in °C. Using the fracture toughness data for a/W= 0.5 provided in Reference [1], T_o is estimated as -129 °C. The corresponding master curve along with the experimental data, converted to 1T equivalent data using Eq. (5), is shown in Figure 3.

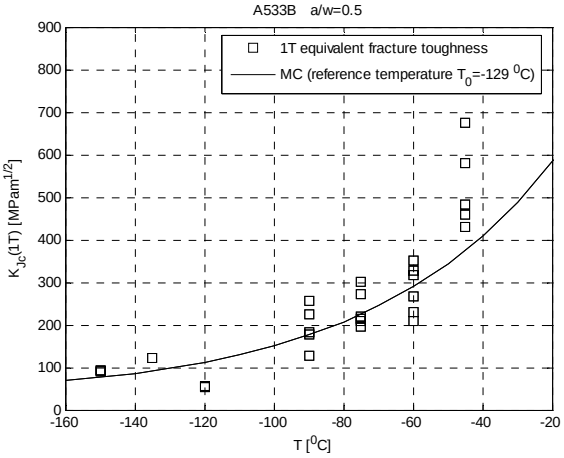

Figure 3 Master curve for specimens with a/W=0.5

In modeling the microscopic fracture process of the metallic materials, it is assumed that the nucleation of microcracks is caused by sufficient stress acting on the brittle cementite leading to slip of the crystalline boundaries due to dislocation motion. As more microcracks are initiated, the nucleation sites may coalesce and form microcrack clusters, which eventually link up with the main crack and the fracture event takes place [3]. Therefore, it can be postulated that fracture occurs when the crack tip opening stress ($\sigma_{\theta\theta}$) reaches or exceeds a critical value (σ_f, or the local fracture stress) at a distance r_c ahead of the crack tip.

In general, the temperature effect is insignificant on local fracture stress [2,3]. For A533B steels, it was found that the local stress σ_f is about 1955 MPa [9,13]. On the other hand, the characteristic distance, r_c, is more sensitive to the temperature variation [14]. The temperature-dependent macroscopic parameters, such as the yield stress, Young's modulus, strain hardening exponent, and the fracture toughness (K_{JC}) for A533B-1 have been determined [1] and shown earlier in Figures 1(a) to 1(d), respectively.

Finite element analyses of three-point bend specimens with a/W= 0.5 at various temperatures are conducted. The specimens are loaded up to J_{IC}, corresponding to the master curve of K_{JC} obtained in Figure 3. The characteristic distance, therefore, can be determined by a given critical stress (σ_f), which for demonstration purpose is chosen as 1955±5% MPa (i.e., 1857.25, 1955, and 2052.75 MPa). The resulting r_c as a function of temperature is plotted in Figure 4.

It can be seen that r_c increases as the temperature rises. This is consistent with the findings for 22NiMoCr3-7 steel (A508) in Reference [14]. This fact can be explained as follows: The lower material yield stress at higher temperature leads to a more extensive crack tip blunting and a larger stretch zone size (SZW) [15]. As a result, the higher crack tip stress relief requires larger fracture process zone so more microcracks can be formed and linked to the main crack.

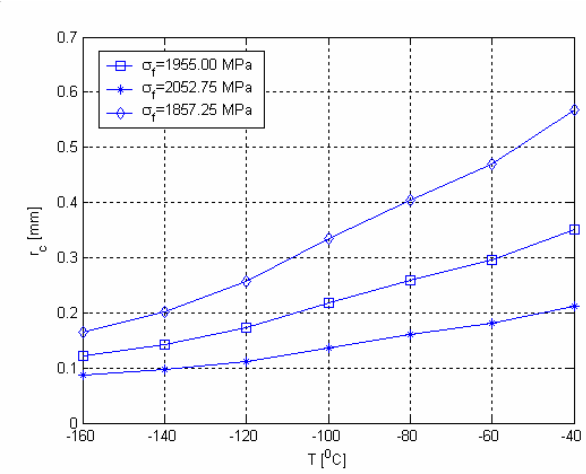

Figure 4 Characteristic distance (r_c) as a function of temperature

Based on the assumption that the fracture initiation is independent of the crack size, it is reasonable to infer that the relationship between the temperature and the characteristic distance, r_c, in Figure 4 can be applied to any ratios of a/W in this study. The test results in Reference [14] appear to support this conclusion.

PREDICTION OF FRACTURE TOUGHNESS IN DUCTILE-BRITTLE TRANSITION ZONE

J-A_2 Two-parameter Constraint Theory in Fracture Mechanics

When the Ramberg-Osgood strain hardening law is used to describe the material constitutive response, the stress-strain relationship can be expressed as

$$\frac{\varepsilon_{ij}}{\varepsilon_0} = (1+\nu)\frac{\sigma_{ij}}{\sigma_0} - \nu\frac{\sigma_{kk}}{\sigma_0}\delta_{ij} + \frac{3}{2}\alpha\left(\frac{\sigma_e}{\sigma_0}\right)^{n-1}\frac{S_{ij}}{\sigma_0} \quad (8)$$

where ν is the Poisson's ratio, δ_{ij} is the Kronecker delta, $S_{ij} = \sigma_{ij} - \sigma_{kk}\delta_{ij}/3$ is the deviatoric stress, and $\sigma_e = \sqrt{3S_{ij}S_{ij}/2}$ is the Mises equivalent stress.

The elastic-plastic stress field for a Mode I crack can be obtained by asymptotic solution. Hutchinson [16,17], Rice, and Rosengren [18] (HRR) used the first term in the series expansion to provide a singular, dominant solution as the crack tip is approached (r→0):

$$\frac{\sigma_{ij}(r,\theta)}{\sigma_0} = \left(\frac{J}{\alpha\varepsilon_0\sigma_0 I_n r}\right)^{1/(n+1)} \tilde{\sigma}_{ij}(\theta,n) \quad (9)$$

where (r, θ) is the polar coordinate of a material point with the origin at the crack tip, J is the J-integral which uniquely defines the magnitude of the crack tip stress, I_n is a non-dimensional integration constant and depends only on the strain hardening exponent n, and $\tilde{\sigma}_{ij}(\theta,n)$ is a non-dimensional stress distribution function.

The constraint effect in fracture mechanics has drawn much of the attention since mid-20th century [19] due to the issues of applying the laboratory determined fracture toughness to full structures (i.e., transferability). Yang et al. [20] and Chao et al. [21] developed the higher order terms in the asymptotic expansion, and concluded that only two parameters (J and A_2) are needed to describe the near crack tip solution:

$$\frac{\sigma_{ij}(r,\theta)}{\sigma_0} = A_1\left[\left(\frac{r}{L}\right)^{S_1}\tilde{\sigma}_{ij}^{(1)}(\theta,n) + A_2\left(\frac{r}{L}\right)^{S_2}\tilde{\sigma}_{ij}^{(2)}(\theta,n) + A_2^2\left(\frac{r}{L}\right)^{S_3}\tilde{\sigma}_{ij}^{(3)}(\theta,n)\right] \quad (10)$$

where L is a characteristic length, which can be regarded as the crack length, specimen width, or a unit length (e.g., unity),

$$A_1 = \left(\frac{J}{\alpha\varepsilon_0\sigma_0 I_n L}\right)^{-S_1}$$

$$S_1 = -\frac{1}{n+1} \quad (11)$$

and $\tilde{\sigma}_{ij}^{(k)}(\theta,n)$ is the non-dimensional stress distribution function with respect to S_k (k= 1, 2, and 3; $S_1 < S_2 < S_3$). When the strain hardening exponent (n) is greater or equal to 3, $S_3 = 2S_2 - S_1$. The stress index S_k is a function of n only, and is independent of the applied load and the material constants, such as α, ε_o, or σ_o in the Ramberg-Osgood power law. In Eqs. (10) and (11), the integration constant I_n , the stress distribution function $\tilde{\sigma}_{ij}^{(k)}(\theta,n)$ and the stress index S_k have been tabulated by Chao and Zhang [22].

It should be noted that the first term in Eq. (10) is the HRR solution (i.e., Eq. (9)). By introducing the second fracture parameter, A_2, the J-A_2 controlled region would be greater than that dominated by the J-integral alone. In this J-A_2 theory, J remains the role in describing the crack tip stress intensity, while A_2 is used to describe the constraint level of the cracked body. The value of A_2 can be obtained by matching the finite element solution to Eq. (10).

Prediction of Fracture Toughness at Various Temperatures

Based on the RKR fracture model [2], the crack initiation takes place when the circumferential stress $\sigma_{\theta\theta}(\theta=0)$ reaches a critical value σ_f in the ligament a distance r_c from the crack tip. From Eq. (10),

$$\sigma_f = \sigma_0\lambda\left(\frac{J_c}{\alpha\varepsilon_0\sigma_0 I_n L}\right)^{-S_1} \quad (12)$$

where

$$\lambda = \left[\left(\frac{r_c}{L}\right)^{S_1}\tilde{\sigma}_{ij}^{(1)}(0,n) + A_2\left(\frac{r_c}{L}\right)^{S_2}\tilde{\sigma}_{ij}^{(2)}(0,n) + A_2^2\left(\frac{r_c}{L}\right)^{S_3}\tilde{\sigma}_{ij}^{(3)}(0,n)\right] \quad (13)$$

It can be seen that λ is a function of crack tip constraint (expressed by A_2) and the material properties.

For a specimen with a given a/W ratio, it is assumed that A_2 is a constant (note that this assumption will be revisited in the next section). Therefore, from Eqs. (12) and (13), the fracture toughness (J_C) in the ductile-brittle transition region can be predicted by

$$J_C = \left(\frac{\lambda\sigma_o}{\sigma_f}\right)^{\frac{1}{S_1}}\varepsilon_o\sigma_o I_n L\alpha \quad (14)$$

To demonstrate the fracture toughness prediction with Eq. (14), finite element analysis is first performed to estimate the A_2 values under fully plastic condition for a/W= 0.5, 0.2, 0.1, and 0.075, which are determined as, respectively, -0.17, -0.23, -0.26, and -0.27. By further assuming that the deep cracks and the shallow cracks follow the same fracture initiation mechanism, a constant fracture stress, σ_f, is applied to all crack sizes (see the paragraph above Figure 3). Therefore, by substituting into Eq. (14) the value of σ_f (in the present work, it appears that the lower bound value, 1857.25 MPa, gives a better prediction), along with the temperature-dependent material parameters (i.e., σ_o and $\varepsilon_o = \sigma_o/E$ in Figs. 1) and r_c (the upper curve in Fig. 4), the corresponding ductile-brittle transition curves (1T K_{JC}) can be obtained for a/W= 0.5, 0.2, 0.1, and 0.075, as shown in Figures 5(a) to 5(d), respectively. It can be seen that the predicted curves in general agree well with the experimental data.

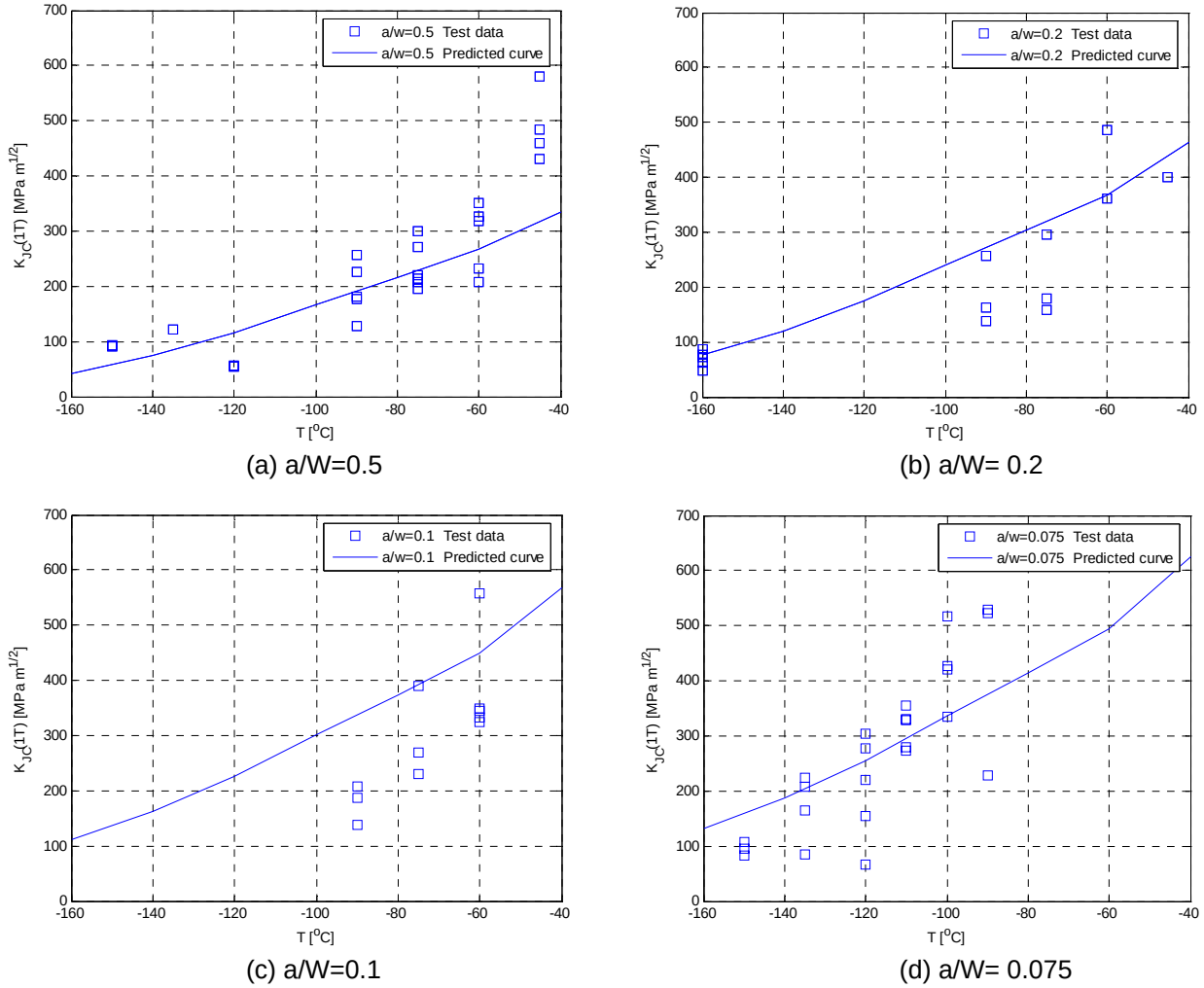

(a) a/W=0.5 (b) a/W= 0.2

(c) a/W=0.1 (d) a/W= 0.075

Figure 5 Predicted fracture toughness (K_{JC}) in ductile-brittle transition temperature regime using σ_f= 1857.25 MPa and the temperature dependent r_c in Figure 4: (a) a/W= 0.5, (b) a/W= 0.2, (c) a/W= 0.1, (d) a/W= 0.075

Discussion of A_2 Dependence on J and Temperature

In the previous section, the constraint parameter A_2 was assumed as a constant for a given a/W, and not to depend on the temperature. However, based on the fact that the material parameters, such as E or n, are functions of temperature (Figs. 1(a) to 1(d)), it is likely that A_2 would be varied with the temperature as well. The A_2 dependence on temperature and on loading level (J-integral) will be discussed in the following.

From the finite element solution, A_2 can be obtained at various loading levels characterized by the J-integral. In the case of a/W= 0.5 at T= -100 °C, this relationship is plotted in Figure 6. It can be seen that A_2 initially increases with the rising load but rapidly approaches a constant value. The same trend can be found for the other crack sizes (a/W). Chao et al. [21] have investigated the A_2 variation with respect to J for different strain hardening exponents, n. They found that the constraint parameter A_2 is indeed a constant value for a given a/W under fully plastic condition. This fact was later theoretically proved by Chao and Zhu [23].

Figure 7 shows the relationship between the constraint parameter A_2 and the temperature in the case of a/W= 0.5. Each A_2 value is estimated at a load level corresponding to the temperature dependent J_C on the mater curve (based on Fig. 3). It can be seen that A_2 is essentially unchanged at low temperatures. However, as the temperature is above -100 °C, the A_2 value tends to be decreased. This may be caused by the stress relief at the crack tip due to the enlarged plastic zone size. However, the effect of decreasing value of A_2 is not expected to be significant on predicting the fracture toughness in ductile-brittle transition.

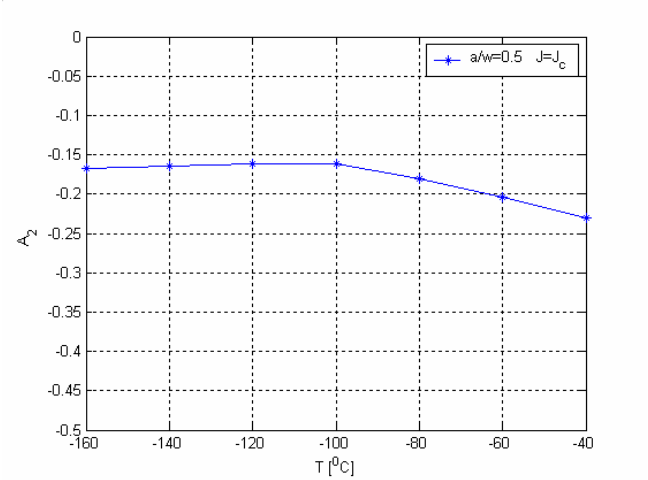

Figure 6 The relationship between the constraint parameter A_2 and the temperature T

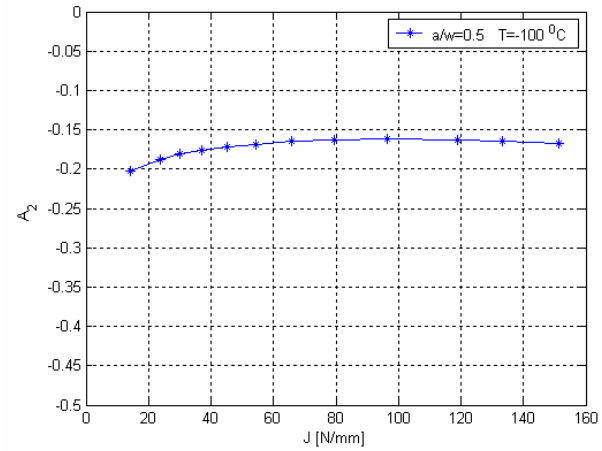

Figure 7 The relationship between the constraint parameter A_2 and the J-integral

CONCLUSIONS

Based on the tensile and fracture toughness data of A533B-1 pressure vessel steel provided by Reference [1] and the finite element analysis using the ABAQUS code [10], the temperature dependant characteristic distance, r_c, is first established based on a constant critical fracture stress of the material, σ_f. By employing the J-A_2 constraint theory in fracture mechanics [20,21], it is shown that the fracture toughness (K_{JC} or J_C) in the ductile–brittle transition temperature regime can be predicted by Eq. (14), which is a function of the critical fracture stress (σ_f), characteristic distance from the crack tip (r_c), loading parameter (J), constraint parameter (A_2), and the tensile properties of the steel. Furthermore, by confirming that the constraint parameter A_2 is insensitive to the temperature and the loading, a conclusion can be made that, for a given crack length to specimen width ratio (i.e., a/W), the fracture toughness throughout the ductile-brittle transition temperature regime can be fully characterized by a single constraint parameter, A_2. The predicted fracture toughness has been shown in good agreement with the experimental data [1].

ACKNOWLEDGEMENT

The authors wish to thank Professor Andrew H. Sherry, Materials Performance Centre at the University of Manchester, United Kingdom, for obtaining the clearance from AEA Technology plc, United Kingdom, for releasing to us their report AEAT/RJCB/RD01329400/R003.

REFERENCES

[1] A. H. Sherry, D. P. G. Lidbury, and D. W. Beardsmore, (2001), "Validation of Constraint-Based Structural Integrity Assessment Methods. Final Report," AEAT/RJCB/RD01329400/R003, AEA Technology plc, UK.

[2] R. O. Ritchie , J. F. Knott, and J. R. Rice, (1973),"On the relationship between critical tensile stress and fracture toughness in mils steel, "Journal of the Mechanics and Physics of Solids, 21, pp. 395-410.

[3] R. O. Ritchie, W. L. Server ,and R. A. Wulleart, (1979), "Critical fracture stress and fracture strain models for prediction of lower and upper shelf toughness in nuclear pressure vessel steel," Metallurgical Transactions, 10A, pp. 1557-1570.

[4] G. Z. Wang, G. H. Liu and J. H. Chen, (2001), "Effects of precracked specimen geometry on local cleavage fracture stress σ_f of low alloy steel", International Journal of Fracture, 112, pp. 183–196.

[5] G. Z. Wang, Y. L. Wang, and J. H. Chen, (2005), "Effects of loading rate on the local cleavage fracture stress σ_f in notched specimens", Engineering Fracture Mechanics 72, pp. 675–689.

[6] J. H. Chen, G. Z. Wang, C. Yan, H. Ma, and L. Zhu, (1997), "Advances in the mechanism of cleavage fracture of low alloy steel at low temperatures. Part. III: Local Fracture Stress σ_f," International Journal of Fracture, 83, pp. 139–157.

[7] G. Z. Wang , J. G. Wang, J. H. Chen, (2003) "Effects of geometry of notched specimens on the local cleavage fracture stress σ_f of C–Mn steel", Engineering Fracture Mechanics 70, pp. 2499–2512.

[8] D. A. Cury and J. F. Knott, (1978), "Effect of microstructure on cleavage fracture stress in steel", Material Science, pp. 511-514.

[9] Z. A. Chen, Z. Zhen and Y. J. Chao, (2007), "Effect of crack depth on the shift of the ductile-brittle transition curve of steels," Engineering Fracture Mechanics, 74, pp. 2437-2448.

[10] ABAQUS, Version 6.6, (2006), Dassault Systèmes Simulia Corp., Providence, Rhode Island, USA.
[11] H. W. Viehrig, J. Boehmert, and J. Dzugan, (2002), "Some issues by using the master curve concept," Nuclear Engineering and Design, 212, pp. 115-124.
[12] ASTM E1921-07, (2007), "Standard Test Method for Determination of Reference Temperature, T_o, for Ferritic Steels in the Transition Range," American Society for Testing and Materials, West Conshohochen, PA.
[13] S. R. Ortner and C. A. Hippsley , (1996), "Two component description of ductile to brittle transition in ferritic steel," Material Science and Technology, 12, pp. 1035-1042.
[14] Jörg Hohe, Jochen Hebel, Valérie Friedmann, and Dieter Siegele, (2007), "Probabilistic failure assessment of ferritic steels using the master curve approach including constraint effects," Engineering Fracture Mechanics 74, pp. 1274 – 1292.
[15] E. Roos, X. Schuler, H. Silcher, H. P. Seebich, and U. Eisele, (2005), "Classification of the master curve concept within the framework of safety assessment based on mechanics of materials," 18th International Conference on Structural Mechanics in Reactor Technology (SmiRT18-G01-4).
[16] J. W. Hutchinson, (1968a), "Singular behavior at the end of a tensile crack in a hardening material," Journal of the Mechanics of Physics and Solids, 16, pp. 13-31.
[17] J. W. Hutchinson, (1968b), "Plastic stress and strain fields at a crack tip," Journal of the Mechanics of Physics and Solids, 16, pp. 337-347.
[18] J. R. Rice and G. F. Rosengren, (1968), "Plane strain deformation near a crack tip in a power-law hardening material," Journal of the Mechanics of Physics and Solids, 16, pp. 1-12.
[19] G. R. Irwin, (1957), "Analysis of stresses and strains near the end of a crack traversing a plate," Journal of Applied Mechanics, 24, pp. 361-364.
[20] S. Yang, Y. J. Chao, and M. A. Sutton, (1993), "Higher-order asymptotic fields in power-law hardening material," Engineering Fracture Mechanics, 45, pp. 1-20.
[21] Y. J. Chao, S. Yang and M. A. Sutton, (1994), "On the fracture of solids characterized by one or two parameters: Theory and Practice," Journal of the Mechanics of Physics and Solids, 42, pp. 629-647.
[22] Y. J. Chao and L. Zhang, (1997), Tables of plane strain crack tip fields: HRR and higher order terms, ME-Report, 97-1, Department of Mechanical Engineering, University of South Carolina, Columbia, SC.
[23] Y. J. Chao and X. K. Zhu, (2000), "Constraint-modified J-R curves and its application to ductile crack growth," International Journal of Fracture, 106, pp. 135-160.